



ELSEVIER

Applied Surface Science 96–98 (1996) 126–130

applied  
surface science

## Preferential vaporization and plasma shielding during nano-second laser ablation

Xianglei Mao <sup>a</sup>, Wing-Tat Chan <sup>b</sup>, Manuel Caetano <sup>c</sup>, Mark A. Shannon <sup>d</sup>,  
Richard E. Russo <sup>a,\*</sup>

<sup>a</sup> Lawrence Berkeley Laboratory, Berkeley, CA 94720, USA

<sup>b</sup> Department of Chemistry, University of Hong Kong, Pokfulam Road, Hong Kong

<sup>c</sup> Escuela de Química, Universidad Central de Venezuela, P.O. Box 47102, Caracas 1020-A, Venezuela

<sup>d</sup> Department of Mechanical Engineering, University of Illinois at Urbana-Champaign, Urbana, IL 61801, USA

Received 22 May 1995

### Abstract

Preferential removal of components from mixed material targets and plasma shielding are studied by using inductively coupled plasma-atomic emission spectrometry (ICP-AES) during UV nano-second laser ablation. The ICP emission intensity for Cu and Zn during ablation of brass samples varies versus laser power density. A model using thermal evaporation and inverse Bremsstrahlung processes is presented. The model shows that plasma shielding occurs at approximately 0.3 GW/cm<sup>2</sup>, in agreement with experimental data for change in the mass ablation rate. The good agreement of model and experimental data suggest that thermal effects are important during nano-second laser ablation for power density less than 0.3 GW/cm<sup>2</sup>.

### 1. Introduction

Laser ablation is a process that involves non-linear coupling of photon energy of a laser beam into the surface of a solid, resulting in evaporation, ejection of electrons, atomic and ionic species, clusters, and fragments. This technology can be used as a solid sampling approach for analytical spectroscopy [1–12] with advantages such as no sample preparation, small sample requirements, spatial analysis, and the ability to analyze directly, any materials. However, fractional vaporization [12–16] in metals occurs, which is dependent on the laser power density.

The thermal component of the interaction influences the quantity and composition of the vapor. In addition, the laser induced surface plasma influences the efficiency of laser energy coupled to the surface, available for material removal.

We report laser ablation of brass with UV nano-second pulsing using inductive coupled plasma-atomic emission spectrometry (ICP-AES). ICP-AES is an excellent technology for studying laser ablation processes at atmosphere pressure. The ablated material is introduced into an Ar (or other inert gas) flow and carried to ICP, where the sampled material is heated and excited to optical emission. The influence of laser beam parameters (pulse width, wavelength, and power density) on the laser material interaction can be investigated. In this paper the emission inten-

\* Corresponding author.

sity of Cu and Zn and their ratio as a function of laser power density was studied during nano-second laser ablation. A model is presented to show that nano-second laser ablation likely involves thermal processes at low power density, which can explain the fractional removal of Zn and Cu.

## 2. Experimental

A diagram of the experimental system is shown in Fig. 1. The system has been previously described in detail [16]. The primary components are an excimer laser ( $\lambda = 248$  nm, pulse width 20 ns), an ICP spectrometer with a photodiode array detector, and a computer with associated data acquisition electronics. The energy of the excimer laser at the sample target was 30 mJ and the pulse rate was 10 Hz.

The laser beam was focused onto the brass samples (35% Zn composition) using a plano-convex lens with a 20 cm focal length. Power density at the sample surface was estimated from the energy of the laser beam, pulse width, and laser beam spot area. The fluence at the target surface is from 2 to 120 J/cm<sup>2</sup>. The ablated vapor is carried by Ar gas into the ICP where it is excited to optical emission. The brass samples were repetitively ablated at each location for 60 seconds before data acquisition to remove surface impurities. Cu emission at 324.75 nm and Zn emission at 334.5 nm were measured. Spectral emission in the ICP is directly related to the mass ablated

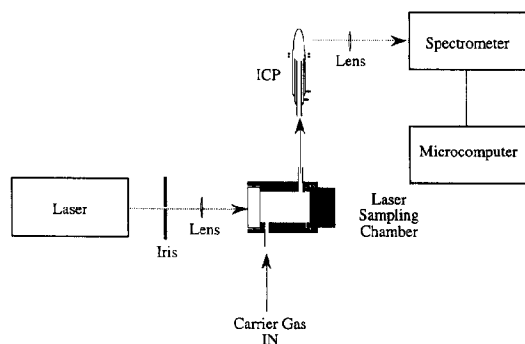


Fig. 1. Experimental configuration for studying laser ablation using ICP-AES.

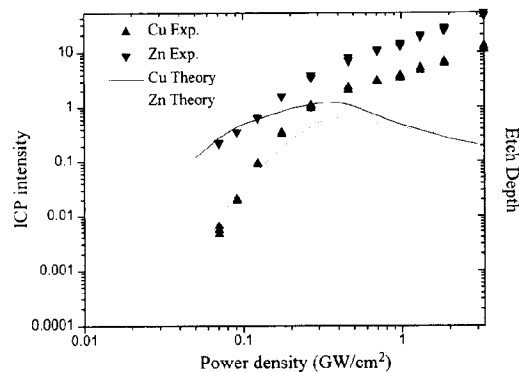


Fig. 2. Experimental data for Cu and Zn emission intensity in ICP normalized to laser beam area as function of laser power density. The curves are calculated etch depth using the model described in the text.

from the target. The ICP emission intensity is normalized to laser beam area in order to obtain the mass ablation rate per unit area.

## 3. Experimental results

The Cu (324.75 nm) and Zn (334.5 nm) emission intensity normalized to laser beam area as a function of laser power density are shown by the data points in Fig. 2. The mass ablation rate increases with laser power density and is proportional to  $P^n$ , where  $n$  depends on the particular element and laser power density range. The mass ablation rate shows a roll-off at approximately 0.3 GW/cm<sup>2</sup>. Also, the change in mass ablation rate for Cu is much greater than that of Zn in the lower power density range, and it is similar after the power density reaches 0.3 GW/cm<sup>2</sup>. As the laser power density increases, the Zn/Cu intensity ratio reduces and reaches a constant level at approximately 0.3 GW/cm<sup>2</sup> (Fig. 3). ICP-AES shows that Zn is enriched at lower power density whereas the composition is close to the original material at higher laser power density, for ns UV laser ablation. These data demonstrate that preferential or non-stoichiometric ablation occurs, dependent on laser power density.

#### 4. Thermal evaporation model

Laser ablation involves complex processes, with many simultaneous mechanisms influencing the amount and composition of the vapor. The surface temperature increases and neutral atoms are evaporated as laser light is absorbed by the target. Photoelectrons are emitted from the surface. These electrons can gain energy from the laser light during collision with atoms and ions (inverse Bremsstrahlung process). Ionization processes begin when kinetic energy of electron is higher than the ionization potential of evaporated atoms. The laser induced plasma above the surface can shield portions of the laser beam during the pulse. We describe a preliminary model based on thermal evaporation and inverse Bremsstrahlung that correlates with our experimental observation of roll off and preferential vaporization, as measure for Zn and Cu in Figs. 2 and 3.

The ablated vapor is described by three components: electrons, ions, and neutral atoms with subscripts e, i, and n, respectively.

The energy of electrons is [17,18]:

$$\varepsilon_e = \frac{3}{2}n_e k_B T_e + n_e k_B \Theta_i \quad (1)$$

where  $T_e$  and  $n_e$  are electron temperature and density.  $\Theta_i$  is the ionization potential. The first term is kinetic energy and second is ionization energy.

The energy of particles (ions and atoms) is:

$$\varepsilon_p = \frac{3}{2}n_p k_B T_p \quad (2)$$

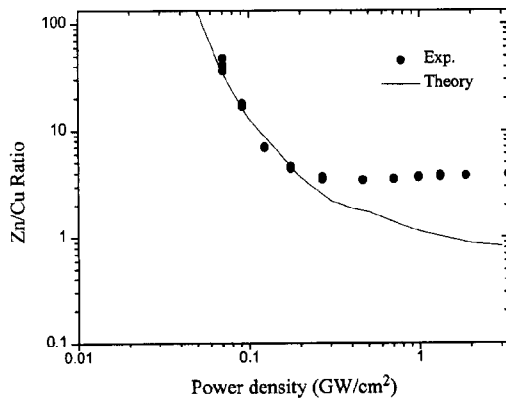


Fig. 3. Experimental data showing the ratio of Zn to Cu emission intensity as function of laser power density. The curves are ratio of Zn to Cu calculated from the model.

where  $T_p$  and  $n_p$  are particle temperature and number density.

Assuming that the electron density and temperature are homogenous in the entire vapor cloud, the change of electron energy should equal to energy absorbed from the laser light minus energy transferred to particles via collision,

$$\frac{d\varepsilon_e}{dt} = \frac{1 - \exp(-Hk_1)}{H} (1 - R)I - \frac{3}{2}k_B \times (T_e - T_p) \nu_{tr} n_e \quad (3)$$

where  $I$  is the laser intensity  $\nu_{tr}$  is the energy transfer frequency.  $k_1$  is the absorption coefficient of the plasma, and  $H$  is the thickness of the plasma.  $R$  is the reflectivity of the target. At  $\lambda = 248$  nm, the reflectivity of Cu is 0.34. The reflectivity of Al decreases to zero during the laser pulse after surface melting start [17]. Therefore, we only consider that  $R$  is equal to zero in this model. By assuming the plume expands with sonic velocity,

$$\frac{dH}{dt} = \sqrt{\frac{\gamma k_B T_p}{M}}, \quad (4)$$

where  $\gamma$  is the ratio of  $C_p$  and  $C_v$ .  $M$  is particle mass. The absorption coefficient from inverse Bremsstrahlung can be defined as [18],

$$k_1 = \frac{3.7 \times 10^8}{\sqrt{T_e} \omega^3} Z^2 \left[ \exp\left(\frac{h\omega}{k_B T_e}\right) - 1 \right] \times n_e n_i + \frac{e^2 \nu_c n_e}{\pi m c \omega^2} \quad (5)$$

where  $\omega$  is the laser frequency,  $Z$  is the ionic charge,  $m$  is electron mass,  $e$  is electron charge,  $c$  is light speed, and the  $n_i$  is number density of ions. The first term in Eq. (5) represents photo absorption from ions whereas the second term is absorption from atoms. The electron-atom collision frequency  $\nu_c$  is

$$\nu_c = n_a \sigma_c \sqrt{\frac{8k_B T_e}{\pi m}} \quad (6)$$

where  $\sigma_c$  is the electron-atom collision cross section and  $n_a$  is the density of atoms.

The change of particle energy equals to the kinetic energy transferred from electrons and the kinetic energy carried by the atoms vaporized from

sample surface. If we assume that the temperature of atoms vaporized from surface is equal to the surface temperature, then

$$\frac{d\varepsilon_p}{dt} = \frac{3}{2}k_B T_s \frac{J_v}{H} + \frac{3}{2}k_B(T_c - T_p)v_{tr}n_e. \quad (7)$$

The ionization rate is:

$$\frac{dn_e}{dt} = \alpha_i n_a n_e - \beta_R n_i n_e^2 \quad (8)$$

where

$$\alpha_i = C_i \sqrt{k_B T_c} \exp(-\Theta_i/T_c) \quad (9a)$$

and

$$\beta_R = C_i \left[ 2 \left( \frac{2\pi m}{h} \right)^{3/2} \left( \frac{g_i}{g_k} \right) kT_c \right]. \quad (9b)$$

$C_i$  is an experimental parameter determined from electron ionization cross section data [19].

For  $Z = 1$  then

$$\begin{aligned} n_e &= n_i, \\ n_p &= n_i + n_a. \end{aligned} \quad (10)$$

The change in number density of atoms in the plasma is equal to atoms evaporated from the surface:

$$\frac{d(H(n_a + n_i))}{dt} = J_v \quad (11)$$

where  $J_v$  is the evaporation rate. Assuming thermal equilibrium [20],

$$J_v = P_v(T_s) \sqrt{\frac{M}{2\pi k_B T_s}} \quad (12)$$

where  $P_v(T_s)$  is the vapor pressure of the target elements.

$$P_v(T_s) = 1.06 \times 10^6 \exp\left(-\frac{L_v}{k_B} \left(\frac{1}{T_s} - \frac{1}{T_B}\right)\right), \quad (13)$$

$L_v$  is the heat of vaporization and  $T_B$  is the boiling-point temperature.

For brass,  $J_v$  will be:

$$\begin{aligned} J_v &= C_{Cu} P_{vCu}(T_s) \sqrt{\frac{M_{Cu}}{2\pi k_B T_s}} \\ &+ (1 - C_{Cu}) P_{vZn}(T_s) \sqrt{\frac{M_{Zn}}{2\pi k_B T_s}} \end{aligned} \quad (14)$$

where  $C_{Cu}$  is the concentration of Cu atoms in the brass alloy. In our sample,  $C_{Cu}$  is approximate 0.65.

We have five differential equations (Eq. (3), (4), (7), (8) and (11)) for  $n_e$ ,  $n_a$ ,  $T_c$ ,  $T_p$ ,  $H$ , and  $T_s$  and six variables. For surface temperature [21],

$$\frac{\partial^2 T(x, t)}{\partial x^2} = \frac{1}{\kappa} \frac{\partial T(x, t)}{\partial t}, \quad x > X(t), t > 0, \quad (15)$$

$$T(x, 0) = T_0,$$

$$T(\infty, t) = T_0,$$

$$-K \frac{\partial T}{\partial x} \Big|_{x=X(t)} = I(t) - \rho L_v \frac{dX(t)}{dt}$$

where  $K$  is the thermal conductivity of the target which is assumed to be constant, and  $\rho$  is the density.  $X(t)$  is the new surface position during evaporation which is determined by  $dX/dt = (1/\rho)J_v(T_s)$ .  $I = \exp(-Hk_1)$  is the effective laser intensity incident on the target surface. By using Eq. (15) we can calculate the surface temperature if we know how much laser light is absorbed, and then estimate how much material is evaporated. By solving these equations, the amount of Cu and Zn evaporated during laser ablation as a function of power density can be calculated. The etch depth is the calculated from total mass of Cu and Zn evaporated

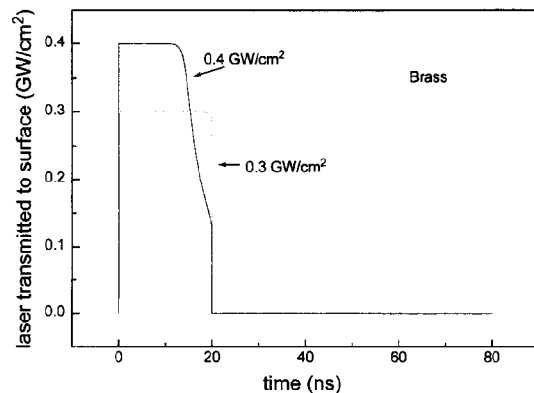


Fig. 4. Laser light transmitted to the target surface as function of time during the laser pulse for two power densities.

per unit area divided by the density of brass. The laser is assumed to be a rectangular pulse with 20 ns duration and power density of 0.3 and 0.4 GW/cm<sup>2</sup>. The laser intensity transmitted to the surface as a function of time was calculated (Fig. 4). This model shows that plasma shielding starts at  $\approx 0.3$  GW/cm<sup>2</sup>, the same power density at which experimental data shows roll-off. The transmitted laser energy to the surface decreases above this power density. The total Cu and Zn evaporated during the laser pulse was integrated from  $J_v(t)$ , and the results are included in Figs. 2 and 3. The calculated ablation rate from the model agrees with experimental data in the lower power density region ( $< 0.3$  GW/cm<sup>2</sup>). Specifically, the model shows different ablation rates for Zn and Cu (and the change in their ratio) and approximately the power density at which roll-off occurs. At higher power density, the mass removal rate is less than the experimental. The model does not consider energy transfer between the hot plasma and sample surface, shock wave interactions, nor numerous other electronic and mechanical effects.

However, using this model, a thermal mechanism appears to play an important role in UV ns-laser ablation. The photon energy of the nanosecond laser pulse is converted to heat instantly in the target and the quantity and composition of the laser ablated vapor is governed by the principle of thermodynamics in the low power density region. At the higher laser power density, the process is more complex and our preliminary model does not apply. The laser induced plasma is not transparent and a significant portion of incident laser energy is absorbed, increasing the temperature and pressure of plasma. The critical point of the solid is reached because of the high temperature and pressure plasma. Once the critical point in the solid is reached the vapor and liquid phases can not be distinguished. The vapor composition could be the same as that in the solid phase and preferential vaporization may be governed by the plasma-surface interaction.

## Acknowledgements

This research was supported by the U.S. Department of Energy, Office of Basic Energy Sciences, Chemical Sciences Division, Processes and Techniques Branch, under Contract No. DE-AC03-76SF00098.

## References

- [1] L. Moenke-Blankenburg, *Spectrochim. Acta Rev.* 15 (1993) 1.
- [2] J.A.C. Broekaert, F. Leis, B. Raeymaekers and G. Zaray, *Spectrochim. Acta* 43B (1989) 339.
- [3] K. Dittrich and R. Wennrich, *Prog. Anal. Atom. Spectrosc.* 7 (1984) 139.
- [4] F. Leis and K. Laqua, *Spectrochim. Acta* 33B (1978) 727.
- [5] P.G. Mitchell, J. Sneddon and L.J. Radziemski, *Appl. Spectrosc.* 40 (1986) 274.
- [6] M. Thompson, J.E. Goulter and F. Sieper, *Analyst* 106 (1981) 32.
- [7] J.W. Carr and G. Horlick, *Spectrochim. Acta* 37B (1982) 1.
- [8] M.E. Tremblay, B.W. Smith, M.B. Leong and J.D. Winefordner, *Spectrosc. Lett.* 20 (1987) 311.
- [9] A.L. Gray, *Analyst* 110 (1985) 551.
- [10] R.E. Russo, X.L. Mao, W.T. Chan, M.F. Bryant and W.F. Kinard, *J. Anal. At. Spectrom.* 10 (1995) 295.
- [11] W.T. Chan and R.E. Russo, *Spectrochim. Acta* 48B (1991) 1471.
- [12] P. Arrowsmith, *Anal. Chem.* 59 (1987) 1437.
- [13] J.W. Hager, *Anal. Chem.* 61 (1989) 1243.
- [14] T. Mochizuki, A. Sakashita, T. Tsuji, H. Iwata, Y. Ishibashi and N. Gunji, *Anal. Sci.* 7 (1991) 479.
- [15] M. Thompson, S. Chenery and L. Brett, *J. Anal. At. Spectrom.* 4 (1989) 11.
- [16] W.T. Chan, X.L. Mao and R.E. Russo, *Appl. Spectrosc.* 46 (1992) 1025.
- [17] I. Ursu, I.N. Mihaiescu, I. Apostol, M. Dinescu, Al Hening, M. Stoica, A.M. Prokhorov, V.P. Ageev, V.I. Konov and V.N. Tokarev, *J. Phys. D: Appl. Phys.* 17 (1984) 1315.
- [18] R.J. Harrach, Rep. No. UCRL-52389, Lawrence Livermore Laboratory, University of California (1987).
- [19] R.S. Freund, R.C. Wetzel, R.J. Shul and T.R. Hayes, *Phys. Rev.* 41A (1990) 3575.
- [20] D.I. Rosen, J. Mitteldorf, G. Kothandaraman, A.N. Pirri and E.R. Pugh, *J. Appl. Phys.* 53 (1982) 3190.
- [21] J.F. Ready, *J. Appl. Phys.* 36 (1965) 462.